

## Video Article

# Recording Gamma Band Oscillations in Pedunculopontine Nucleus Neurons

Francisco J Urbano<sup>1</sup>, Brennon R Luster<sup>2</sup>, Stasia D'Onofrio<sup>2</sup>, Edgar Garcia-Rill<sup>2</sup><sup>1</sup>IFIBYNE-CONICET, University of Buenos Aires<sup>2</sup>Center for Translational Neuroscience, University of Arkansas for Medical SciencesCorrespondence to: Edgar Garcia-Rill at [garciarilledgar@uams.edu](mailto:garciarilledgar@uams.edu)URL: <http://www.jove.com/video/54685>DOI: [doi:10.3791/54685](https://doi.org/10.3791/54685)Keywords: Arousal, Ca<sup>2+</sup> channels, gamma oscillations, N-Type, P/Q-type, current ramps

Date Published: 6/20/2016

Citation: Urbano, F.J., Luster, B.R., D'Onofrio, S., Garcia-Rill, E. Recording Gamma Band Oscillations in Pedunculopontine Nucleus Neurons. *J. Vis. Exp.* (), e54685, doi:10.3791/54685 (2016).

## Abstract

Synaptic efferents from the PPN are known to modulate the neuronal activity of several intralaminar thalamic regions (e.g., the centrolateral/parafascicular; Cl/Pf nucleus). The activation of either the PPN or Cl/Pf nuclei *in vivo* has been described to induce the arousal of the animal and an increment in gamma band activity in the cortical electroencephalogram (EEG). The cellular mechanisms for the generation of gamma band oscillations in Reticular Activating System (RAS) neurons are the same as those found to generate gamma band oscillations in other brains nuclei. During current-clamp recordings of PPN neurons (from parasagittal slices from 9-25 day-old rats), the use of depolarizing square steps rapidly activated voltage-dependent potassium channels that prevented PPN neurons from being depolarized beyond -25 mV.

Injecting 1-2 sec long depolarizing current ramps gradually depolarized PPN membrane potential resting values towards 0 mV. However, injecting depolarizing square pulses generated gamma-band oscillations of membrane potential that showed to be smaller in amplitude compared to the oscillations generated by ramps. All experiments were performed in the presence of voltage-gated sodium channels and fast synaptic receptors blockers. It has been shown that the activation of high-threshold voltage-dependent calcium channels underlie gamma-band oscillatory activity in PPN neurons. Specific methodological and pharmacological interventions are described here, providing the necessary tools to induce and sustain PPN subthreshold gamma band oscillation *in vitro*.

## Introduction

PPN nucleus is anatomically included in the caudal mesencephalic tegmentum. The PPN is a key component of RAS<sup>1</sup>. The PPN participates in the maintenance of behavioral activated states (i.e., waking, REM sleep)<sup>2</sup>. Electrical stimulation of the PPN *in vivo* induced fast oscillation (20-40 Hz) in the cortical EEG<sup>3</sup>, while bilateral PPN lesions in the rat reduced or eliminated REM sleep<sup>4</sup>. While a majority of PPN neurons fire action potentials at beta/gamma-band frequency (20-80 Hz), some neurons presented low rates of spontaneous firing (<10 Hz)<sup>5</sup>. Furthermore, the PPN seems to be involved in other aspects of behavior such as motivation and attention<sup>6</sup>. Direct high frequency (40-60 Hz)<sup>7</sup> electrical stimulation of PPN nucleus in decerebrate animals can promote locomotion. In recent years, deep brain stimulation (DBS) of PPN has been used to treat patients suffering from disorders involving gait deficits such as Parkinson's disease (PD)<sup>8</sup>.

Previous reports demonstrated that almost all PPN neurons can fire action potentials at gamma band frequency when depolarized using square current pulses<sup>9</sup>. Because of the drastic activation of voltage-gated potassium channels during square pulses depolarizations up to or under -25 mV. As a consequence, no robust gamma oscillations were observed after blocking action potentials generation using tetrodotoxin<sup>10</sup>. In an effort to bypass such a problem, 1-2 sec long depolarizing current ramps were used. Ramps gradually depolarized the membrane potential from resting values up to 0 mV, while partially inactivating voltage-gated potassium channels. Clear gamma band membrane oscillations were evident within the voltage dependence window of high threshold calcium channels (i.e., between -25 mV and -0 mV)<sup>10</sup>. In conclusion, gamma band activity was observed in PPN neurons<sup>9</sup>, and both P/Q- and N-type voltage-gated calcium channels need to be activated in order to generate gamma band oscillations in the PPN<sup>10</sup>.

A series of studies determined the location of high threshold calcium channels in PPN neurons. Injecting the combination of dyes, *ratiometric* fluorescence imaging showed calcium transients through voltage-gated calcium channels that are activated in different dendrites when depolarized using current ramps<sup>11</sup>.

Intrinsic properties of PPN neurons have been suggested to allow simultaneous activation of these cells during waking and REM sleep, thus inducing high-frequency oscillatory neuronal activity between the RAS and thalamocortical loops. Such long-reaching interaction is considered to support a brain state capable of reliably assessing the world around us on a continuous basis<sup>12</sup>. Here, we describe the experimental conditions necessary to generate and maintain gamma band oscillation in PPN cells *in vitro*. This protocol has not been described previously, and would help a number of groups to study intrinsic membrane properties mediating gamma band activity at other brain areas. Moreover, current steps might lead to the erroneous conclusion that gamma band activity cannot be generated in these cells.

## Protocol

All experimental protocols were approved by the Institutional Animal Care and Use Committee of the University of Arkansas for Medical Sciences (Protocol number #3593) and were in agreement with the National Institutes of Health guidelines for the care and use of laboratory animals.

### 1. Preparation of standard-artificial cerebrospinal fluid (aCSF)

#### 1. Preparation of Stock Solution A

1. Add 700 mL of distilled water to a clean 1 liter beaker before adding chemicals.
2. While continuously stirring a volume of 500 mL, add 136.75 g of NaCl, 6.99 g of KCl, 2.89 g of MgSO<sub>4</sub>, and 2.83 g of NaH<sub>2</sub>PO<sub>4</sub>.
3. Add more distilled water to reach a final volume of 1 liter. After dilution, the final concentration of each compound is 117 mM NaCl, 4.69 mM KCl, 1.2 mM MgSO<sub>4</sub>, and 1.18 mM NaH<sub>2</sub>PO<sub>4</sub>.
4. Keep refrigerated at 4 °C for up to 2 weeks.

#### 2. Preparation of Stock Solution B

1. Add 700 mL of distilled water to a clean 1 liter beaker before adding chemicals.
2. While continuously stirring a volume of 500 mL, add 41.45 g of D-glucose and 41.84 g of NaHCO<sub>3</sub>.
3. Add more distilled water to reach a final volume of 1 liter. After dilution, the final concentration of each compound is 11.5 mM D-glucose and 24.9 mM NaHCO<sub>3</sub>.
4. Keep refrigerated at 4 °C for up to 2 weeks.
5. Before each experiment mix 50 mL of stock A with 50 mL stock B and bring to 1 liter with distilled water to obtain final concentration aCSF solution and leave at room temperature while continuously oxygenating it with carbogen (95% O<sub>2</sub>-5% CO<sub>2</sub> mix) for at least 30 minutes. Prepare final concentration aCSF only at the beginning of each experiment and discard at the end of the day.

### 2. Preparation of sucrose-artificial cerebrospinal fluid (sucrose-aCSF)

#### 1. Preparation of Stock Solution C

1. Add 700 mL of distilled water to a clean 1 liter beaker before adding chemicals.
2. While continuously stirring 500 mL of distilled water, add 240 g of sucrose, 6.55 g of NaHCO<sub>3</sub>, 0.671 g of KCl, 4.88 g of MgCl<sub>2</sub>, 0.22 g of CaCl<sub>2</sub> and 0.21 g of ascorbic acid.
3. Add more distilled water to reach a final volume of 1 liter. After dilution, the final concentration of each compound is 701.1 mM sucrose, 78 mM NaHCO<sub>3</sub>, 9 mM KCl, 24 mM MgCl<sub>2</sub>, 1.5 mM CaCl<sub>2</sub> and 1.2 mM ascorbic acid.
4. Keep stock solution C at 4 °C for up to one week.
5. Before each experiment mix 300 mL of 50 mL of stock C with 600 mL distilled water to obtain the sucrose-aCSF solution at the final concentration and leave at room temperature while continuously oxygenating it with carbogen (95% O<sub>2</sub>-5% CO<sub>2</sub> mix) for at least 30 minutes.

### 3. Slice preparation

1. Place a clean beaker with 100 mL sucrose-aCSF solution in ice while oxygenating it with carbogen and fix the pH at 7.4 using a pH meter while adding few drops of 0.1 M NaOH solution (when pH < 7.4) or 0.1 M HCl solution (when pH > 7.4).
2. Fill up a cutting chamber of a vibratome with sucrose-aCSF and oxygenate it. Turn on the glycerol-based refrigerating system coupled to the cutting chamber and wait 15 minutes to allow it to cool down to 0-4 °C.
3. Anesthetize rat pups (aged 9 to 12 from adult timed-pregnant Sprague-Dawley rats) with Ketamine (70 mg/kg, *i.p.*; using <50 µL final volume). When pup is calm, double check that tail pinch reflex is absent.
4. Decapitate pups.
  1. Cut the head skin longitudinally from the front to back using a carbon steel scalpel blade, and pull the skin to the sides using forceps. Cut the bone covering the brain moving the scissors laterally and totally remove it to expose the brain.
  2. Then, rapidly remove the brain using a spatula (initially placed under the olfactory bulb in order to gently push out the brain from the most rostral towards the most caudal areas). Gently push the brain into ice-cooled oxygenated sucrose-artificial cerebrospinal fluid (sucrose-aCSF).
5. Make a parasagittal cut on the right hemisphere (removing approximately one third of the hemisphere), and glue the trimmed side of the brain onto a metallic disk that will be magnetically fixed to the cutting chamber of a vibroslicer to cut sagittal 400 µm sections containing the pedunculo-pontine nucleus (PPN). Keep PPN slices at room temperature for 45 minutes prior to whole-cell patch-clamp recordings.

### 4. Recordings gamma-band oscillations in PPN slices

#### 1. Preparation of potassium-gluconate intracellular solution (high-K<sup>+</sup> solution).

1. Place in ice a clean beaker with 10 mL distilled water. While continuously stirring add: K<sup>+</sup>-gluconate, 90.68 mg phosphocreatine di Tris salt, 47.66 mg HEPES, 1.5 mg EGTA, 40.58 mg Mg<sup>2+</sup>-ATP, and 4 mg Na<sup>+</sup><sub>2</sub>-GTP.
2. Adjust pH to 7.3 with KOH (100 mM in distilled water). Add distilled water to reach a final volume of 20 mL. If needed, adjust osmolarity with sucrose (100 mM in distilled water) to be 280-290 mOsm. After dilution, the final concentration of each compound is 124 mM K<sup>+</sup>-gluconate, 10 mM phosphocreatine di Tris salt, 10 mM HEPES, 0.2 mM EGTA, 4 mM Mg<sup>2+</sup>-ATP, and 0.3 mM Na<sup>+</sup><sub>2</sub>-GTP.

3. Aliquot intracellular solutions in 1 mL tubes and freeze at -20 °C. Use one aliquot per day and keep at 4 °C during experiments.

## 2. Whole-cell patch clamp recordings

1. Place slices in an immersion chamber and perfuse them (1.5 mL/min) with oxygenated (95% O<sub>2</sub>- 5% CO<sub>2</sub>) aCSF containing the following receptor antagonists: selective NMDA receptor antagonist 2-amino-5-phosphonovaleric acid (APV, 40 μM), competitive AMPA/Kainate glutamate receptor antagonist 6-cyano-7-nitroquinoxaline-2,3-dione (CNQX, 10 μM), glycine receptor antagonist strychnine (STR, 10 μM), the specific GABA<sub>A</sub> receptor antagonist gabazine (GBZ, 10 μM), and sodium channel blocker tetrodotoxin (TTX, 3 μM)  
NOTE: In the results and figures, these antagonists are collectively referred to as synaptic blockers or SBs.
2. Fill the recording patch pipettes (Resistance 2-7 MΩ; made from regular, commercially available thick wall borosilicate glass capillaries of 1.0 mm outer diameter and 0.6 mm inner diameter) with intracellular high-K<sup>+</sup> solution using commercially available patch-pipette fillers with a solution filter. Insert the pipette in its amplifier's holder. Apply a small positive pressure using a 1 mL syringe connected to the pipette holder using a silicon tube connected to a three-way valve. Connect the back of the pipette holder to a patch clamp amplifier.
3. Move the recording pipette using a mechanical micromanipulator near the PPN nucleus using a 4X objective combined to near-infrared differential interference contrast optics.  
NOTE: PPN nucleus can be observed in slices dorsal to the superior cerebellar peduncle (SCP; observable as a thick bundle of axons). Recording pipettes were located in the PPN *pars compacta*, which is located immediately dorsal to the posterior end of the peduncle.
4. Bring the recording pipette in contact with a PPN neuron while visualized using a 40x water immersion lens, and rapidly apply negative suction to form a seal with the cell.
5. Use voltage-clamp seal software to monitor pipette resistance during negative suction using manufacturer's protocol.
  1. When negative suction is slowly increased and resistance values reading by the patch-clamp monitor at the tip of the pipette reach 80-100 MΩ, rapidly change the holding potential to -50 mV and release the negative pressure. Start continuously applying negative suction until rupturing the neuron's membrane and electrical access is achieved in the whole-cell configuration.
  2. If access resistance values measured by the voltage-clamp seal software are 10 MΩ or higher, then continue applying negative suction in smaller amounts.
6. Compensate capacitance (i.e., slow and fast transients observed after rupturing the membrane of the cell) and series resistance in voltage-clamp mode. Switch recording mode to current clamp, and rapidly compensate bridge values (e.g., move amplifier knob or click on the automatic compensation menu using computer's mouse).
  1. Continuously monitor resting membrane potential of PPN neuron being recorded using manufacturer's protocol. If resting membrane potential shift towards depolarizing or hyperpolarizing values, then use small amounts of direct current (up to 100 pA) to keep the optimum -50 mV final value.  
NOTE: Keep only PPN neurons with a stable resting membrane potential (RMP) of -48 mV or more hyperpolarized (i.e., RMP < -48 mV).

## Representative Results

Initially, gamma oscillations were evoked using square current pulses. Current clamp recording of PPN neurons in the presence of synaptic blockers and TTX was continuously monitored to assure that resting membrane potential was kept stable at ~-50 mV (Figure 1A). Two second long square current pulses were injected intracellularly by the patch clamp amplifier through the recording pipette, increasing their amplitude from 200 pA to 600 pA (Figure 1A). Membrane potential was depolarized to voltage levels closer to -20 mV when 600 pA, resulting in small amplitude gamma oscillations. Powers spectra of gamma oscillations presented very small amplitude values (i.e., <0.01; Figure 1B). On the other hand, two second depolarizing current ramps was injected intracellularly by the patch clamp amplifier through the recording pipette, generating robust gamma oscillations (Figure 2A) that presented much higher *power* amplitudes (Figure 2B).

Previous work<sup>10</sup> has linked differences between square and ramp current protocols to the string activation of voltage-gated potassium channels during sudden depolarization of the former. Slow depolarizing ramps might instead be inactivating potassium channels.

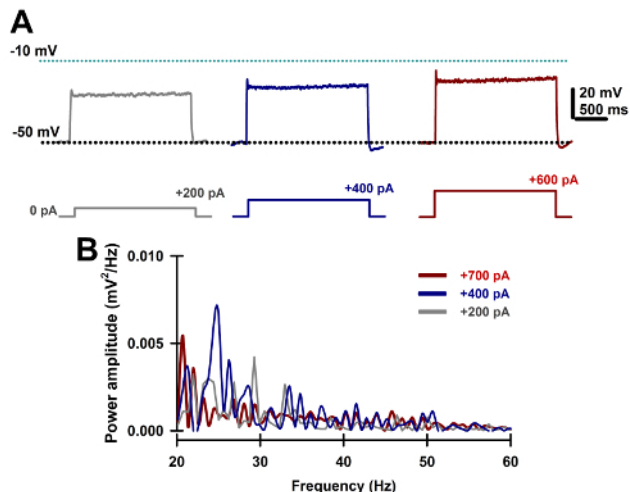


**Figure 1. Membrane oscillations in whole-cell recorded PPN neurons using current square pulses of increasing amplitude. A.** Representative membrane potential responses to depolarizing 2 second long square steps of increasing amplitude injected intracellularly by the patch clamp amplifier through the recording pipette, in the presence of synaptic blockers and TTX. **B.** Overlapping power spectra amplitudes for oscillations obtained using square pulses shown in A. Power spectra were obtained using a Hamming window function after 20-60 Hz bandpass filtering oscillations generated by the depolarizing steps. PPN neuron was recorded in current-clamp configuration combining high-K<sup>+</sup> intracellular solution and synaptic blockers + TTX described in Protocol. [Please click here to view a larger version of this figure.](#)

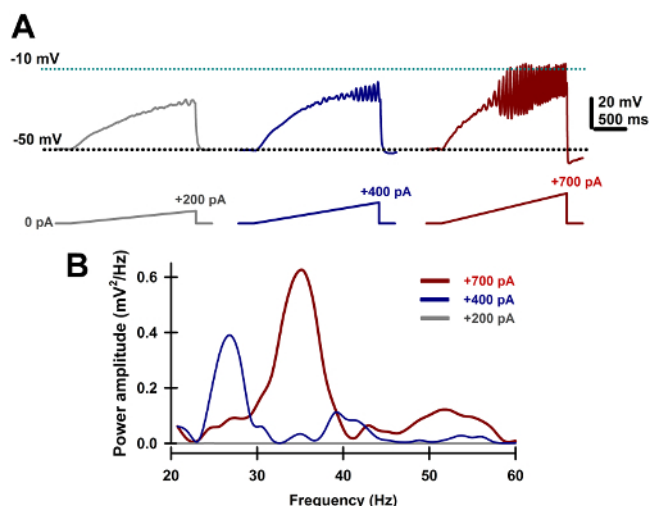


**Figure 2. Gamma band membrane oscillations in whole-cell recorded PPN neurons using current ramps of augmenting amplitude. A.** Representative membrane potential responses to depolarizing 2 second long ramps injected by the patch clamp amplifier intracellularly through the recording pipette, showing increasing amplitude in the presence of synaptic blockers and TTX. **B.** Overlapping power spectra amplitudes for oscillations obtained using ramps shown in A. Power spectra were obtained using a Hamming window function after 20-60 Hz bandpass filtering oscillations generated by the depolarizing ramp. PPN neuron was recorded in current-clamp configuration combining high-K<sup>+</sup> intracellular solution and synaptic blockers + TTX described in Protocol. [Please click here to view a larger version of this figure.](#)

## Discussion

PPN neurons have intrinsic properties that allow them to fire action potentials at beta/gamma band frequencies during *in vivo* recordings from animals that are awake or during REM sleep, but not during slow wave sleep<sup>2,3,5,13-17</sup>. Other authors have showed that brainstem transections at more anterior levels than PPN reduced gamma frequencies during EEG recordings. However, when brainstem lesions posterior to where this nucleus is located, the direct stimulation of PPN allowed the manifestation of cortical gamma activity on the EEG<sup>2,3,5,18-21</sup>. Gamma band neural activity has been reported in the mouse PPN *in vitro*<sup>22</sup>, in the rat REM sleep-induction area (to which the PPN projects<sup>23</sup>), in the cat *in vivo*<sup>3</sup>, in the PPN area in primates when locomoting<sup>24</sup>, and in the region of the PPN in humans during stepping<sup>25</sup>. That is, there is ample evidence for gamma band activity in the PPN across species.

This experimental protocol detailed here permitted the description of gamma oscillations present at all rat PPN cell types<sup>10</sup>. In fact, intrinsic mechanisms underlying gamma oscillations were described to be present in every PPN neuron (while cells around the PPN do not share that property), regardless of previous used classifications or synaptic transmitter type: type I, II, or III, or transmitter type, cholinergic, glutamatergic or GABAergic share the same gamma-band generating property<sup>10</sup>. The use of current ramps has the limitation of requiring continuous monitoring of the resting membrane potential, and permanent bridge compensation throughout the experiment. In some cases, ramps shorter than 1 sec were

observed to not fully activate voltage-gated calcium channels, while ramp durations of 5 sec or longer resulted in membrane resistance changes that would remain uncompensated during the experiment. In case no gamma oscillations were observed, small adjustments in ramp duration could enhance gamma band oscillation amplitudes.

Combining depolarizing current-ramps with specific toxins we have described that in an important proportion of PPN cells (~50%) blocking N- and P/Q-type (using both  $\omega$ -CgTx and  $\omega$ -Aga) channels calcium channels reduced gamma oscillation amplitude, which allow us to classified them as P/Q- and N-type cells. In other cells (20%), gamma oscillations were only affected by  $\omega$ -Aga, suggesting that these cells expressed only P/Q-type channels. In the rest of the cells (30%) only  $\omega$ -CgTx blocked them, suggesting these PPN neurons had only N-type channels. These results confirmed the presence of cells in the PPN that manifest gamma band oscillations through the expression of different voltage-gated calcium channels<sup>26,27</sup>. This new protocol can also be considered a key tool that allowed the introduction of a new PPN cell type classification to the field. In fact, it has been suggested that N-type only PPN neurons fire only during REM sleep ("REM-on"), P/Q-type only during waking ("Wake-on"), or N-type + P/Q-type during both waking and REM sleep ("Wake/REM-on")<sup>26,27</sup>. Furthermore, this protocol might be used in future experiments to describe oscillatory activity at other brain areas and to demonstrate the intrinsic properties triggering them.

## Disclosures

The authors declare that they have no competing financial interests.

## Acknowledgements

This work was supported by core facilities of the Center for Translational Neuroscience supported by NIH award P20 GM103425 and P30 GM110702 to Dr. Garcia-Rill. This work was also supported by grants from FONCYT-Agencia Nacional de Promoción Científica y Tecnológica; BID 1728 OC.AR. PICT-2012-1769 and UBACYT 2014-2017 #20120130101305BA (to Dr. Urbano).

## References

1. Profice, P., *et al.* Neurophysiological evaluation of the pedunculopontine nucleus in humans. *J. Neural. Transm (Vienna)*. **118** (10), 1423-1429 (2011).
2. Steriade, M., Datta, S., Pare, D., Oakson, G., & Curro Dossi, R.C. Neuronal activities in brain-stem cholinergic nuclei related to tonic activation processes in thalamocortical systems. *J. Neurosci.* **10** (8), 2541-2559 (1990).
3. Steriade, M., Dossi, R.C., Pare, D., & Oakson, G. Fast oscillations (20-40 Hz) in thalamocortical systems and their potentiation by mesopontine cholinergic nuclei in the cat. *Proc. Natl. Acad. Sci. U.S.A.* **88** (10), 4396-4400 (1991).
4. Deurveilher, S., & Hennevin, E. Lesions of the pedunculopontine tegmental nucleus reduce paradoxical sleep (PS) propensity: evidence from a short-term PS deprivation study in rats. *Eur. J. Neurosci.* **13** (10), 1963-1976 (2001).
5. Steriade, M., Pare, D., Datta, S., Oakson, G., & Curro Dossi, R. Different cellular types in mesopontine cholinergic nuclei related to pontogeniculo-occipital waves. *J. Neurosci.* **10** (8), 2560-2579 (1990).
6. Steckler, T., Inglis, W., Winn, P., & Sahgal, A. The pedunculopontine tegmental nucleus: a role in cognitive processes? *Brain Res. Brain Res. Rev.* **19** (3), 298-318 (1994).
7. Garcia-Rill, E., Simon, C., Smith, K., Kezunovic, N., & Hyde, J. The pedunculopontine tegmental nucleus: from basic neuroscience to neurosurgical applications: arousal from slices to humans: implications for DBS. *J. Neural. Transm.* **118** (10), 1397-1407 (2011).
8. Mazzone, P., *et al.* Implantation of human pedunculopontine nucleus: a safe and clinically relevant target in Parkinson's disease. *Neuroreport*. **16** (17), 1877-1881 (2005).
9. Simon, C., *et al.* Gamma band unit activity and population responses in the pedunculopontine nucleus. *J. Neurophysiol.* **104** (1), 463-474 (2010).
10. Kezunovic, N., Urbano, F.J., Simon, C., Hyde, J., Smith, K., & Garcia-Rill, E. Mechanism behind gamma band activity in pedunculopontine nucleus (PPN). *Eur. J. Neurosci.* **34** (3), 404-415 (2011).
11. Hyde, J.R., Kezunovic, N., Urbano, F.J., & Garcia-Rill E. Spatiotemporal properties of high speed calcium oscillations in the pedunculopontine nucleus. *J. Appl. Physiol (1985)*. **115** (9), 1402-1414 (2013).
12. Llinas, R.R., Leznik, E., & Urbano, F.J. Temporal binding via cortical coincidence detection of specific and nonspecific thalamocortical inputs: a voltage-dependent dye-imaging study in mouse brain slices. *Proc. Natl. Acad. Sci. U.S.A.* **99** (1), 449-454 (2002).
13. Boucetta, S., Cisse, Y., Mainville, L., Morales, M., & Jones, B.E. Discharge profiles across the sleep-waking cycle of identified cholinergic, gabaergic, and glutamatergic neurons in the pontomesencephalic tegmentum of the rat. *J. Neurosci.* **34** (13), 4708-4727 (2014).
14. Datta, S., & Siwek, D.F. Single cell activity patterns of pedunculopontine tegmentum neurons across the sleep-wake cycle in the freely moving rats. *J. Neurosci. Res.* **70** (4), 79-82 (2002).
15. Datta, S., Siwek, D.F., & Stack, E.C. Identification of cholinergic and non-cholinergic neurons in the pons expressing phosphorylated cyclic adenosine monophosphate response element-binding protein as a function of rapid eye movement sleep. *Neuroscience*. **163** (1), 397-414 (2009).
16. Kayama, Y., Ohta, M., & Jodo, E. Firing of 'possibly' cholinergic neurons in the rat laterodorsal tegmental nucleus during sleep and wakefulness. *Brain Res.* **569** (2), 210-220 (1992).
17. Sakai, K., El Mansari, M., & Jouvet, M. Inhibition by carbachol microinjections of presumptive cholinergic PGO-on neurons in freely moving cats. *Brain Res.* **527** (2), 213-223 (1990).
18. Lindsley, D.B., Bowden, J.W & Magoun, H.W. Effect upon the EEG of acute injury to the brainstem activating system. *Electroenceph. Clin. Neurophysiol.* **1** (4), 475-486 (1949).
19. Moruzzi, G. The sleep-waking cycle. *Ergeb. Physiol.* **64.**, 1-165 (1972).
20. Moruzzi, G., & Magoun, H.W. Brain stem reticular formation and activation of the EEG. *Electroenceph. Clin. Neurophysiol.* **1** (4), 455-473 (1949).

21. Steriade, M., Constantinescu, E., & Apostol, V. Correlations between alterations of the cortical transaminase activity and EEG patterns of sleep and wakefulness induced by brainstem transections. *Brain Res.* **13** (1), 177-180 (1969).
22. Ishibashi, M., *et al.* Orexin receptor activation generates gamma band input to cholinergic and serotonergic arousal system neurons and drives an intrinsic  $Ca^{2+}$ -dependent resonance in LDT and PPT cholinergic neurons. *Frontiers Neurol.* **6**, e120 (2015).
23. Brown, R.E., Winston, S., Basheer, R., Thakkar, M.M., & McCarley, R.W. Electrophysiological characterization of neurons in the dorsolateral pontine REM sleep induction zone of the rat: intrinsic membrane properties and responses to carbachol and orexins. *Neuroscience.* **143** (3), 739-755 (2006).
24. Goetz, L., *et al.* On the role of the pedunculo pontine nucleus and mesencephalic reticular formation in locomotion in non-human primates. *J. Neurosci.* **36** (18), 4917-4929 (2016).
25. Fraix, V., *et al.* Pedunculo pontine nucleus area oscillations during stance, stepping and freezing in Parkinson's disease. *PLOS ONE.* **8** (12), e83919, (2013).
26. Luster, B., Hyde, J., D'Onofrio, S., Urbano, F.J., & Garcia-Rill, E. Mechanisms behind gamma band activity in the pedunculo pontine nucleus (PPN). *Abstr Soc Neurosci.* **38**, 257.20 (2014).
27. Luster, B., D'Onofrio, S., Urbano, F.J., & Garcia-Rill, E. High-threshold  $Ca^{2+}$  channels behind gamma band activity in the pedunculo pontine nucleus (PPN). *Physiol. Rep.* **3** (6), e12431 (2015).